

**Short communication**

**Intracranial pressure changes during mouse development**

**Mehran Moazen<sup>1</sup>, Ali Alazmani<sup>2</sup>, Katherine Rafferty<sup>3</sup>, Zi-Jun Liu<sup>3</sup>, Jennifer Gustafson<sup>4</sup>,  
Michael L Cunningham<sup>4</sup>, Michael J Fagan<sup>5</sup>, Susan W Herring<sup>3</sup>**

<sup>1</sup>Department of Mechanical Engineering, University College London, Torrington Place,  
London WC1E 7JE, UK

<sup>2</sup>Institute of Functional Surfaces, School of Mechanical Engineering, University of Leeds,  
Leeds, LS2 9JT, UK

<sup>3</sup>Department of Orthodontics, University of Washington, Seattle, WA 98195-7446, USA

<sup>4</sup>Seattle Children's Research Institute, Center for Developmental Biology & Regenerative  
Medicine and Seattle Children's Craniofacial Center, Seattle, WA 98105, USA

<sup>5</sup>Medical and Biological Engineering, School of Engineering, University of Hull, Hull, HU6  
7RX, UK

Corresponding author:

Mehran Moazen, BSc, PhD, CEng, MIMechE, FHEA

Department of Mechanical Engineering,

University College London,

Torrington Place,

London WC1E 7JE, UK

Tel: +44 (0) 208 954 8056; Fax: +44 (0) 208 954 6371

Email: Mehran\_Moazen@yahoo.com; M.Moazen@ucl.ac.uk

Word count (Introduction through Discussion): 2005

© 2016, Elsevier. Licensed under the Creative Commons Attribution-NonCommercial-  
NoDerivatives 4.0 International <http://creativecommons.org/licenses/by-nc-nd/4.0/>

**Abstract:**

During early stages of postnatal development, pressure from the growing brain as well as cerebrospinal fluid, i.e. intracranial pressure (ICP), load the calvarial bones. It is likely that such loading contributes to the peripheral bone formation at the sutural edges of calvarial bones, especially shortly after birth when the brain is growing rapidly. The aim of this study was to quantify ICP during mouse development. A custom pressure monitoring system was developed and calibrated. It was then used to measure ICP in a total of seventy three wild type mice at postnatal (P) day 3, 10, 20, 31 and 70. Retrospectively, the sample in each age group with the closest ICP to the average value was scanned using micro-computed tomography to estimate cranial growth. ICP increased from  $1.33\pm 0.87$  mmHg at P3 to  $1.92\pm 0.78$  mmHg at P10 and  $3.60\pm 1.08$  mmHg at P20. In older animals, ICP plateaued at about 4 mmHg. There were statistically significant differences between the ICP at the P3 vs. P20, and P10 vs. P20. In the samples that were scanned, intracranial volume and skull length followed a similar pattern of increase up to P20 and then plateaued at older ages. These data are consistent with the possibility of ICP being a contributing factor to bone formation at the sutures during early stages of development. The data can be further used for development and validation of computational models of skull growth.

**Key words:** Intracranial pressure, Skull, Suture, Biomechanics, Development

**Introduction:**

During early stages of postnatal development, intracranial pressure (ICP), from the growing brain and cerebrospinal fluid load calvarial bones and sutures (Moss, 1954; Cohen, 1993; Opperman, 2000; Herring, 2008). It is likely that such loading contributes as an epigenetic factor to the peripheral bone formation at the edges of calvarial bones just after birth. Once forceful mastication starts, muscles also load the craniofacial system and presumably influence cranial growth (Nakata, 1981; Rafferty and Herring, 1999; Al Dayeh et al., 2013). While there is a large ongoing effort to understand the genetic causes of various craniofacial developmental disorders (e.g. Morriss-Kay and Wilkie, 2005; Richtsmeier and Flaherty, 2013; Cox et al., 2013), understanding epigenetic factors such as biomechanical loading based on ICP during normal and abnormal development is crucial too. A broad understanding of the various factors involved in the development of the craniofacial system can in the long term enhance the treatment of various congenital diseases such as craniosynostosis and Treacher Collins syndrome.

Quantifying ICP in infants is clearly challenging, but animal models can provide invaluable insights. In particular, accurate invasive but accurate methods can be employed, rather than non-invasive methods that are safer for children but inadequate for this study (Silasi et al., 2009; Raboel et al., 2012; Murtha et al., 2012; Uldall et al., 2014). Mice are particularly useful in that like other mammals, they have many similarities to humans in terms of calvarial morphology and genome (Morriss-Kay and Wilkie, 2005), their genetics is well characterized and there are models available to investigate the pathogenesis of various craniofacial deformities. Despite a long-standing interest in skull development in mice (e.g. Fong et al., 2003; Henderson, et al., 2005) and rats (e.g. Jones et al., 1987), to the best of our knowledge, intracranial pressure during normal mouse development has not been quantified previously. Such data can be used to enhance our understanding of the biomechanics of normal calvarial growth and possibly, ultimately, management of related congenital

diseases. Therefore, the aims of this study were to develop a suitable ICP measurement system and quantify ICP during wild type mouse development. To highlight morphological changes during development one sample per age group was scanned and analysed.

### **Materials and Methods:**

A pressure monitoring system was developed to measure ICP in mice of 5 age groups. ICP was recorded while animals were anaesthetised. Following the recording animals were decapitated while still under anaesthesia. Then, the sample with closest ICP to the average ICP for each age group was selected for morphological analysis.

**Pressure monitoring system:** A 22-gauge needle (outer diameter 0.70 mm; length 6 mm) was connected via luer-lock to silicone tubing (outer diameter 4 mm; length 250 mm) which was then connected to a differential pressure sensor (TruStability® Board Mount Pressure Sensors: HSC Series, Honeywell, NJ, USA). The measurement range of the sensor was  $\pm 18.68$  mmHg with total error band of 0.19 mmHg. The signal, i.e. changes in the voltage due to external pressure at the tip of the needle, was acquired at 100 Hz using a custom program written in LabVIEW 2013 (National Instruments Corp, Austin, TX, USA). The pressure measurement system was calibrated using tubes with 50, 70, 100, 120 and 150 mm of water, with each test repeated five times.

**In vivo recording of ICP:** A total of seventy-three inbred wild type mice (*Mus musculus*, C57BL/6J - Jackson Labs, Bar Harbor, Maine, USA) at postnatal (P) day 3 ( $2.23 \pm 0.27$  g), 10 ( $5.05 \pm 1.1$  g), 20 ( $9.06 \pm 1.48$  g), 31 ( $17.75 \pm 1.91$  g) and 70 ( $22.46 \pm 4.01$  g) were used. Sex was not recorded for the younger groups, but a retrospective statistical analysis comparing the ICP between males and females at P31 did not show a significant difference. The P70 mice were all female. All protocols were approved by the Institutional Animal Care and Use Committees of the University of Washington and Seattle Children's Research Institute. Mice

were anesthetized using isoflurane in a non-rebreathing custom set-up. During testing heat support was provided via a warm water pad. Once the animals did not respond to toe pinch, a sagittal incision was made over the calvaria. The needle was inserted through the left parietal bone ca. 2 mm lateral to the sagittal suture and 2 mm anterior to the lambdoid suture. With care it was possible to penetrate the bone with the needle even in older animals, but it was important not to enlarge the hole beyond its diameter. The needle was inserted to a depth calculated to position it in the subarachnoid space, which is filled with cerebrospinal fluid. No external pressure was applied to the skull once the needle had been inserted. It was held in place until ICP reached a maximum (typically 1-2 min); when ICP began to drop, or after several minutes if it did not drop, the needle was removed and the maximum recorded pressure was reported. Once recording was completed, the animals were decapitated while still under anaesthesia.

**Statistical analysis:** Statistical analysis was performed in SPSS (IBM SPSS, NY, USA). One-way analysis of variance (ANOVA) with post-hoc Bonferroni and Tukey tests was carried out, with Levene's test used to test for equal variances. The significance level was set at  $p < 0.05$ .

**Ex vivo micro-computed tomography:** The specimen with measured ICP closest to the average ICP value of each age group was scanned using an X-Tek HMX 160 micro-CT scanner (XTek Systems Ltd, Hertfordshire, UK) with a voxel size of 0.01mm in x, y, and z directions. AVIZO (FEI Visualization Sciences Group, Merignac Cedex, France) was used to reconstruct three dimensional models. The scans were automatically aligned with respect to each other in AVIZO based on minimization of the root mean square distance between the nodes forming the triangulated surfaces of the skull (i.e., Procrustes method) using an iterative closest point algorithm. Each skull surface was typically consisted of about 300,000 nodes. Skull length, width and intracranial volume (ICV) were measured using the software.

## **Results:**

**Sensor calibration:** As the needle was gradually moved down the tube of water, voltage gradually increased, plateauing at the bottom of the tube. Similarly, upon removal from the water, voltage decreased to its baseline value (Fig 1A). Calibration of the sensor at various heights of water (each repeated five times) showed that the corresponding voltage changes were stable, repeatable and linear (Fig 1B). Note the error bars corresponding to one standard deviation (of five repeats) are shown in Fig 1B. These values were in the range of 0.004-0.01 V. These calibration data were used to convert the voltage changes during ICP measurement to mmHg.

**ICP Measurements:** ICP was  $1.33\pm 0.87$  mmHg at P3, increasing to  $1.92\pm 0.78$  mmHg at P10,  $3.60\pm 1.08$  mmHg at P20,  $3.81\pm 1.14$  mmHg at P31 and  $4.11\pm 0.83$  mmHg at P70. There were statistically significant differences between P3 vs. P20, P31, P70, and P10 vs. P20, P31, P70, but not between P20, P31 and P70 (Fig 2).

**Morphological changes:** Skull length was 13 mm in the P3 skull and 17, 19, 20 and 22 mm at P10, P20, P31 and P70 respectively. Skull width increased to a lesser extent from 8 mm at P3 to 11 mm at P70. ICV increased from 240 mm<sup>3</sup> at P3 to 339, 462, 474 and 504 mm<sup>3</sup> at P10, P20, P31 and P70 respectively (Fig 3).

## **Discussion:**

Intracranial pressure may be an important factor contributing to calvarial bone formation at the cranial sutures during early postnatal stages of development. In this study ICP during mouse development was quantified at several postnatal ages in a relatively large number of specimens (10-20 at each age). These ages were chosen to capture various stages of development from just after birth (P3) to juvenile (P10 and P20) to early adulthood (P30 and

P70 - see e.g. Hill et al., 2008; Flurkey et al., 2007). Notably, the majority of volumetric brain growth in mice occurs by P20 with lesser increase during P30-P80 (e.g. Zhang et al., 2005). Despite the initial calibration test and repeatability of the results, it is important to compare the ICP data with the existing literature. While no data exist on ICP during mouse development, several studies have quantified ICP in adult mice. Oshio et al. (2004) reported ICP of  $6.99 \pm 1.03$  mmHg in the lateral ventricle (P56-70; n=6), Feiler et al. (2010) reported ICP of  $5.0 \pm 0.5$  mmHg in the epidural space (body weight 23-25 g; n=6), and Yang et al. (2008) reported ICP of  $4.33 \pm 0.62$  mmHg (P70; n=7). Our location, chosen to correspond with our ongoing biomechanical studies on the frontoparietal region (e.g. Moazen et al., 2015), is close to that examined by Yang et al. (2008) i.e. 1 mm posterior to the coronal suture and 1 mm lateral to the sagittal suture. ICP recorded for P70 mice in this study was  $4.11 \pm 0.83$  mmHg (n=13), well within the range of data reported by Yang et al. (2008). This is reassuring, as it validates the ability of our sensor to produce reasonable and reliable data for the younger ages in the present study.

The data obtained showed that ICP increases from about 1.3 mmHg in P3 to 3.6 mmHg in P20 to a limit of approximately 4 mmHg in mice older than P20. This finding is similar to that of Mooney et al. (1998) who measured epidural ICP during rabbit development and reported an increase in ICP from  $3.24 \pm 0.36$  mmHg at P25 (n=28) to  $5.68 \pm 0.38$  mmHg at P42 (n=21). Our morphological measurements are also in agreement with literature (e.g. Zhang et al., 2005; Aggarwal et al., 2009; Chuang et al., 2011). For example, our ICVs of 240, 461 and 504 mm<sup>3</sup> at P3, P20 and P70 are comparable to the values of 200, 400 and 430 mm<sup>3</sup> reported by Chuang et al. (2011) in C57BL/6 mice at the same ages.

ICP, ICV and skull length measurements followed a very similar pattern, with a sharp increase from P3 to P20 and then a plateau. In fact, the majority of bone deposition at the cranial sutures occurs by P20. However, while none of the sutures fully fuse, except for

posterior frontal at about P10, most sutures narrow down to micrometer gaps at P20.

Nonetheless, intrinsic mechanical properties of the bone (approximately 4, 6 and 10 GPa at P10, P20 and P70 respectively) and its thickness (approximately 30, 50 and 150  $\mu\text{m}$  at P10, P20 and P70 respectively) continue to increase (Moazen et al., 2015).

These data together highlight that, development of the brain, intracranial volume, intracranial pressure and also perhaps bone mechanical properties are coupled. These changes occur synchronously until the brain approximates adult size at P20, whereupon ICV and ICP plateau, while bone elastic properties increasingly rigidify the skull (Moss, 1954). While the data do not speak directly to the issue of whether ICP influences bone apposition at the sutural margins (or is influenced by that apposition), they do suggest that the growth of the neurocapsular matrix is not a response to overly high ICP, but rather that ICP rises when the cranium slows its volumetric growth.

There were several limitations in this study. Firstly, it was not possible for us to visualize the insertion of the needle into the skull, nor its final position. Therefore, we cannot be confident that needle was in the subarachnoid space in all cases. However, an atlas of the developing mouse (Aggrawal et al., 2009) was used to plan the needle insertion at various ages, and the single operator (MM) was careful to insert the needle to the pre-identified depths to reach the subarachnoid space. Secondly, animals were anesthetized using isoflurane, and this might have had an impact on ICP (see e.g. Campkin, 1984; Scheller et al., 1987).

Nonetheless, the same procedure was applied to all animals, so the pattern of recorded ICP in this study should remain valid. Finally, we cannot eliminate the possibility of a sex difference in ICP because of missing data. However, at P31 there was no apparent effect of sex.



In summary, this study quantified the changes in intracranial pressure during postnatal development of the mouse. The results showed that ICP increases from about 1.3 mmHg at P3 to 4 mmHg at P31, where it plateaus. These data can be used in computational models of skull growth, allowing the strain patterns in the bone and sutures to be quantified.

### **Conflict of interest**

The authors confirm that there is no conflict of interest in this manuscript.

### **Acknowledgements**

This work was supported by the Royal Academy of Engineering Research Fellowship (MM) and the Jean Renny Endowment for Craniofacial Medicine (MLC). We also thank Dr. Gerry Hish for advice and assistance during this work.

### **References:**

1. Al Dayeh, A.A., Rafferty, K.L., Egbert, M., Herring, S.W., 2013. Real-time monitoring of the growth of the nasal septal cartilage and the nasofrontal suture. *Am J Orthod Dentofacial Orthop.* 143(6), 773-783.
2. Aggarwal, M., Zhang, J., Miller, M.I., Sidman, R.L., Mori, S., 2009. Magnetic resonance imaging and micro-computed tomography combined atlas of developing and adult mouse brains for stereotaxic surgery. *Neuroscience.* 162(4),1339-1350.
3. Campkin, T.V., 1984. Isoflurane and cranial extradural pressure a study in neurosurgical patients. *Br J Anaesth.* 56, 1083-1087.

4. Chuang, N., Mori, S., Yamamoto, A., Jiang, H., Ye, X., Xu, X., Richards, L.J., Nathans, J., Miller, M.I., Toga, A.W., Sidman, R.L., Zhang, J., 2011. An MRI-based atlas and database of the developing mouse brain. *Neuroimage*. 54(1), 80-89.
5. Cohen, M.M. 1993. Sutural biology and the correlates of craniosynostosis. *Am. J. Med. Genet.* 47, 581-616.
6. Cox, T.C., Luquetti, D.V., Cunningham, M.L., 2013. Perspectives and challenges in advancing research into craniofacial anomalies. *Am. J. Med. Genet. C Semin. Med. Genet.* 163C:213-217.
7. Feiler, S., Friedrich, B., Schöller, K., Thal, S.C., Plesnila, N., 2010. Standardized induction of subarachnoid hemorrhage in mice by intracranial pressure monitoring. *J.Neurosci. Methods.* 190(2), 164-170.
8. Flurkey, K., Currer, J.M., Harrison, D.E., 2007. Mouse models in aging research. In: Fox, J.G., et al. (Eds.), *The mouse in biomedical research-Volume 3 normative biology, husbandry, and models*. Academic Press, Burlington MA., pp. 637-670.
9. Fong, K.D., Warren S.M., Loba, E.G., Henderson, J.H., Fang, T.D., Cowan, C.M., Carter, D.R., Longaker, M.T., 2003. Mechanical strain affects dura mater biological processes: implications for immature calvarial healing. *Plast. Reconstr. Surg.* 112(5), 1312-1327.
10. Henderson, J.H., Nacamuli, R.P., Zhao, B., Longaker, M.T., Carter, D.R., 2005. Age-dependent residual tensile strains are present in the dura mater of rats. *J R Soc Interface* 2(3), 159-167.

11. Herring, S.W., 2008. Mechanical influences on suture development and patency. *Front. Oral. Biol.* 12, 41–56.
12. Hill, J.M., Lim, M.A., Stone M.M., 2008. Developmental milestones in the newborn mouse. In: Gozes I (Ed), *Neuropeptide techniques*. Humana Press Inc., Totowa NJ., pp.131-149.
13. Jones, H.C., Deane, R., Bucknall, R.M, 1987. Developmental changes in cerebrospinal fluid pressure and resistance to absorption in rats. *Brain Res.* 430(1), 23-30.
14. Moazen, M., Peskett, E., Babbs, C., Pauws, E., Fagan, M.J., 2015. Mechanical properties of calvarial bones in a mouse model for craniosynostosis. *PloS One.* 10(5), e0125757.
15. Mooney, M.P., Siegel, M.I., Burrows, A.M., Smith, T.D., Losken, H.W., Dechant, J., Cooper, G., Fellows-Mayle, W., Kapucu, M.R., Kapucu, L.O., 1998. A rabbit model of human familial, nonsyndromic unicoronal suture synostosis. II. Intracranial contents, intracranial volume, and intracranial pressure. *Childs Nerv Syst.* 14(6), 247-255.
16. Morriss-Kay, G.M., Wilkie, A.O.M., 2005. Growth of the normal skull vault and its alteration in craniosynostosis : insights from human genetics and experimental studies. *J. Anat.* 207, 637–653.

17. Moss, M.L., 1954. Growth of the calvaria in the rat: the determination of osseous morphology. *Am. J. Anat.* 94,333-361.
18. Murtha, L., McLeod, D., Spratt, N., 2012. Epidural intracranial pressure measurement in rats using a fiber-optic pressure transducer. *J. Vis. Exp.* 62. pii: 3689.
19. Nakata, S., 1981. Relationship between the development and growth of cranial bones and masticatory muscles in postnatal mice. *J. Dent. Res.* 60(8), 1440-1450.
20. Opperman, L.A., 2000. Cranial Sutures as intramembranous bone growth sites. *Dev. Dyn.* 485, 472–485.
21. Oshio, K., Watanabe, H., Song, Y., Verkman, A.S., Manley, G.T., 2005. Reduced cerebrospinal fluid production and intracranial pressure in mice lacking choroid plexus water channel Aquaporin-1. *FASEB J.* 19(1), 76-8.
22. Raboel, P.H., Bartek, Jr. J., Andresen, M., Bellander, B.M., Romner, B., 2012. Intracranial pressure monitoring: invasive versus non-invasive methods - a review. *Crit. Care Res. Pract.* 950393: 14 pages.
23. Richtsmeier, J.T., Flaherty, K., 2013. Hand in glove: brain and skull in development and dysmorphogenesis. *Acta Neuropathol.* 125(4), 469-489.
24. Rafferty, K.L., Herring, S.W., 1999. Craniofacial sutures: morphology, growth and in vivo masticatory strains. *J Morph.* 242,167-179.

25. Scheller, M.S., Todd, M.M., Drummond, J.C., Zornow, M.H., 1987. The intracranial pressure effects of isoflurane and halothane administered following cryogenic brain injury in rabbits. *Anesthesiology*. 67, 507-512.
26. Silasi, G., MacLellan, C.L., Colbourne, F., 2009. Use of telemetry blood pressure transmitters to measure intracranial pressure (ICP) in freely moving rats. *Curr Neurovasc Res*. 6(1), 62-69.
27. Uldall, M., Juhler, M., Skjolding, A.D., Kruuse, C., Jansen-Olesen, I., Jensen, R., 2014. A novel method for long-term monitoring of intracranial pressure in rats. *J. Neurosci. Methods*. 227, 1-9.
28. Yang, B., Zador, Z., Verkman, A.S., 2008. Glial cell aquaporin-4 overexpression in transgenic mice accelerates cytotoxic brain swelling. *J. Biol. Chem*. 283(22), 15280-15286.
29. Zhang, J., Miller, M.I., Plachez, C., Richards, L.J., Yarowsky, P., van Zijl, P., Mori, S., 2005. Mapping postnatal mouse brain development with diffusion tensor microimaging. *NeuroImage*. 26, 1042-1051.

## Figures legend

**Fig 1:** (A) Testing of the pressure sensor with varying heights of water. The needle was slowly inserted to the bottom of a tube of water, held there for 10-25 sec, and then slowly removed. (B) Calibration of the pressure sensor showed the response was linear. Small brackets indicate the SD of measurements.

**Fig 2:** Changes in intracranial pressure during wild type mouse development (means and SDs). The shaded areas indicate ICP data for all samples in the corresponding age group. Asterisks show statistically significant differences.

**Fig 3:** (A) A P70 mouse, highlighting the sagittal and coronal planes used for length and width comparisons. (B) Sagittal and (C) coronal sections of one animal per age. Note the P10 skull became slightly deformed following the ICP measurement and prior to micro-CT scanning. (D) Skull length, width and (E) intracranial volume at P3, P10, P20, P31 and P70.

Fig 1

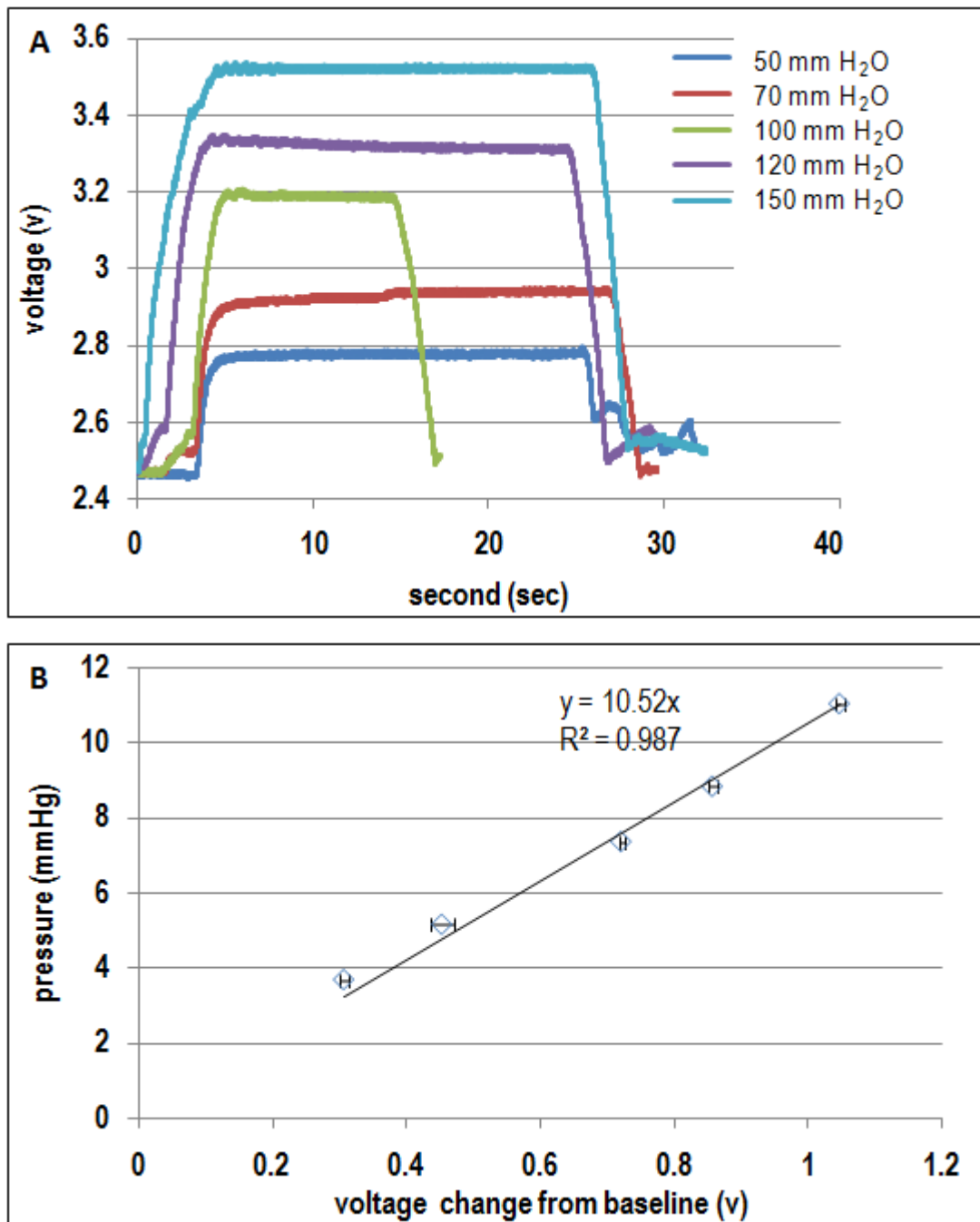


Fig 2

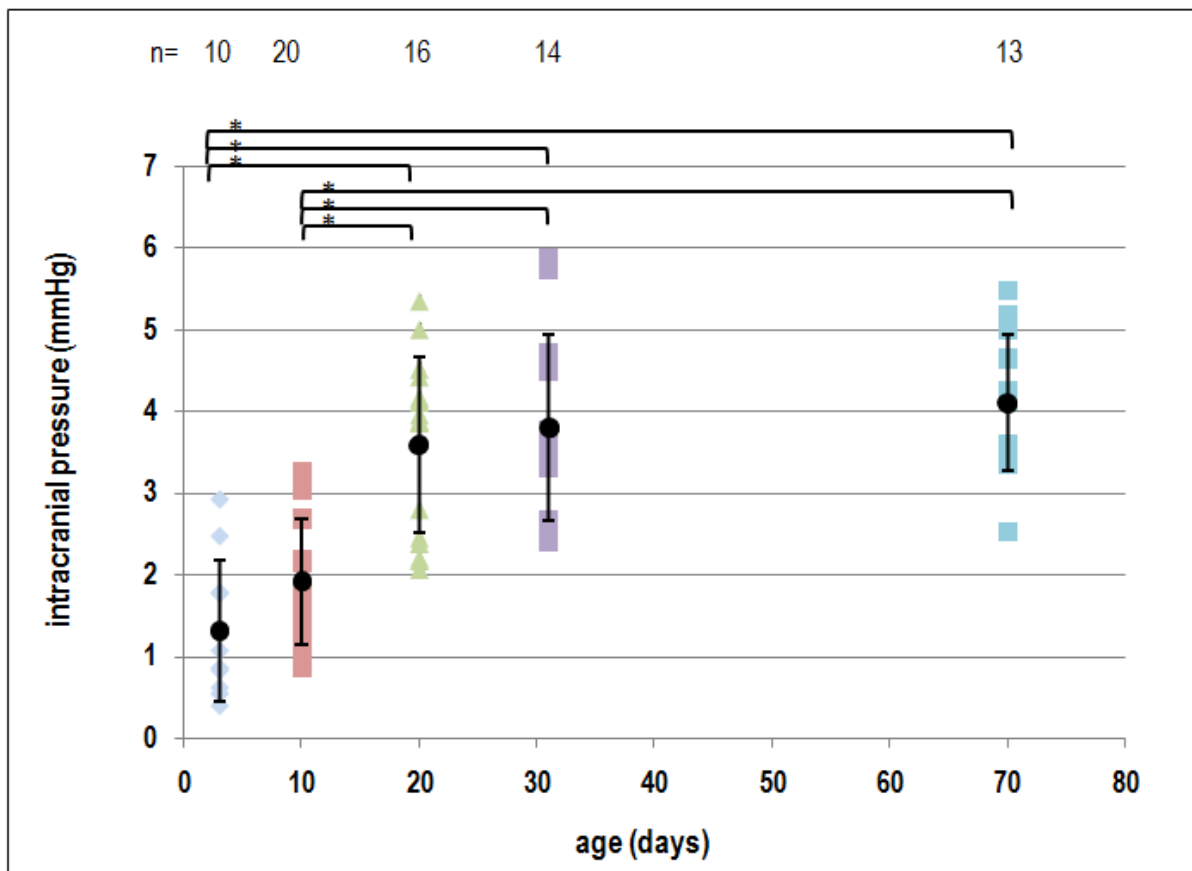




Fig 3

